Development of MOSFET Module SAM4L10M30Z1 for 48V Automotive

Seiji Suzuki*

Abstract

In recent years, the electrification of automobiles has led to the development of various powertrains. Among them, 48V mild hybrid electric vehicles (48V MHEVs), which are in high demand particularly in Europe, have attracted attention. Sanken Electric (hereinafter referred to as "the Company") has developed a 100V low-voltage three-phase MOSFET module, SAM4L10M30Z1, designed for use in electric compressors installed in 48V MHEVs. To achieve both the required performance and compact packaging, it is essential to reduce the on-resistance of the MOSFET and optimize the module's package structure. This paper introduces the performance and development status of this product, which is currently under development.

1. Introduction

As automotive electrification progresses, long-term forecasts suggest a continued shift toward electric vehicles (EVs). In the short term, however, while environmental awareness has led to resistance against internal combustion engine vehicles (ICEs), concerns over the high cost and limited driving range of battery electric vehicles (BEVs) have caused some users to hesitate in purchasing them. As a result, demand for hybrid electric vehicles (HEVs) has been increasing to meet these needs. Among them, 48V mild hybrid electric vehicles (48V MHEVs), which use a 48V power supply, are particularly popular in Europe.

Globally, voltages above DC60V are considered hazardous to the human body and are subject to strict safety standards, which in turn increase costs. Therefore, 48V MHEVs were developed under the concept of reducing CO_2 emissions while keeping costs low. To enter this MHEV market, which can also accommodate future fluctuations in BEV demand, the Company has developed the 100V low-voltage three-phase MOSFET module SAM4L10M30Z1.

In developing this product, customers have requested a compact module package. To meet this requirement, it is necessary to reduce the on-resistance of the MOSFET to support high current while minimizing chip size, and to adopt a package structure with excellent heat dissipation.

This paper discusses the background of the low on-resistance MOSFET and high heat dissipation package design, as well as the product's performance, features, and development status.

2. Market Background

As of 2025, the production ratio of powertrains in the automotive market (see Figure 1) shows that ICEs account for approximately 60% of total vehicle production. In contrast, the combined share of BEVs, range extender EVs (REEV), and fuel cell electric vehicles (FCEVs) is slightly less than 20%. The remaining slightly more than 20% is occupied by other powertrain types, indicating that ICEs still dominate production.

Future projections suggest a gradual shift toward electrification through 2033, and the market for MHEVs, which are the target of this product, is expected to grow steadily. Furthermore, by around 2027, the share of electrified vehicles is forecasted to surpass that of ICEs.

* Engineering Development Headquarters, Power Module Development Division, Intelligent Power Module Development Department, Development Section 2

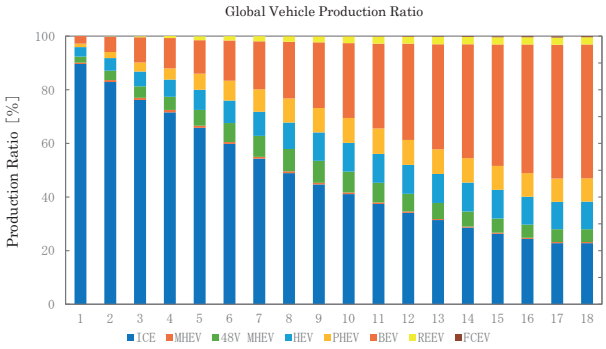

Figure 1. Forecast of Global Vehicle Production Ratio by Powertrain (2023–2033)

Source: Data prepared by MarkLines, "Forecast of Powertrain Composition Ratios in Global Light Vehicle Sales" (Accessed October 2025) [1]

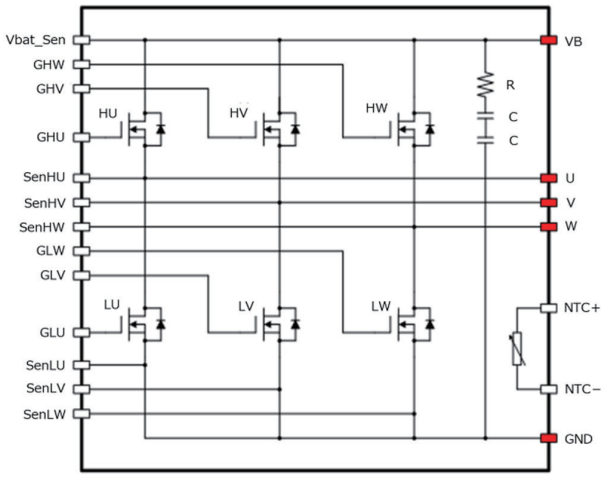

Figure 3. Internal Block Diagram

3. Product Overview

The development concept of this product is to expand the Company's portfolio for automotive applications using 48V power systems, while also addressing potential fluctuations in future BEV demand. The target application is 48V automotive compressors, and the product is a low-voltage three-phase MOSFET module incorporating six low-voltage power MOSFET elements. The specifications of this product are shown in Tables 1, 2, and 3, and Figures 2 and 3.

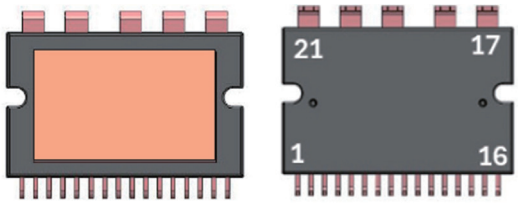

Figure 2. External Appearance Illustration

4. Product Features

This section describes the key features of the product, including the low on-resistance of the MOSFET, functional characteristics, and package design.

4.1 Low On-Resistance MOSFET

The Company's proprietary "ZeroMos" technology improves the trade-off between epitaxial layer resistance (*R*epi) and breakdown voltage, enabling compliance with low on-resistance requirements. Figure 4 illustrates the structure of ZeroMos[2]. A key feature is the formation of a Vertical Field Plate (VFP) with source potential beneath the gate electrode. This structure mitigates the electric field in the epitaxial layer, significantly reducing on-resistance.

Table 1. Absolute Maximum Ratings

T_A = 25℃

symbol	Parameter	SAM4L10M30Z1	unit
V_{DS}	Drain-to-Source Voltage	100	V
V_{GS}	Gate-to-Source Voltage	±20	V
E_{AS}	Single Pulse Avalanche Energy (I_{AS} = 50A)	T.B.D.	mJ
T_j(max)	Maximum Operating Junction Temperature	175	℃
T_{STG}	Storage Temperature	−45 to 175	℃
V_{ISO}(RMS)	Isolation Voltage	2500	V

Table 2. Electrical Characteristics

T_A = 25℃

symbol	Parameter	Condition	SAM4L10M30Z1			unit
			Min	Typ	Max	
BV_{DSS}	Drain-Source Breakdown Voltage	I_D = 1mA, V_{GS} = 0V	(100)	—	—	V
I_{DSS}	Drain-Source Leakage Current	V_{DS} = 100V, V_{GS} = 0V	—	—	(5)	μA
I_{GSS}	Gate-Source Leakage Current	V_{GS} = ±20V	—	—	(±100)	nA
$V_{GS(TH)}$	Gate Threshold Voltage	V_{DS} = 10V, I_D = 1mA	(2.0)	(3.0)	(4.0)	V
$R_{DS(ON)}$ HV	Drain-Source On-Resistance (High-Side V Phase)	I_D = 150A, V_{GS} = 10V	—	(2.05)	(2.75)	mΩ
V_{DS}	Drain-Source Diode Forward Voltage Drop	V_{GS} = 0V, I_S = 100A	—	(0.85)	(1.3)	V
$R\Theta_{JC}$	Junction-to-Case Thermal Resistance	—	—	(0.26)	(0.36)	℃/W

Table 3. Pin Assignment

Pin Number	Pin Name	Function
1	NTC+	NTC Thermistor Pin 1
2	NTC−	NTC Thermistor Pin 2
3	SenLW	Low-Side W-Phase Sense Pin
4	GHW	High-Side W-Phase Gate Pin
5	SenHW	High-Side W-Phase Sense Pin
6	GLW	Low-Side W-Phase Gate Pin
7	SenLV	Low-Side V-Phase Sense Pin
8	GHV	High-Side V-Phase Gate Pin
9	SenHV	High-Side V-Phase Sense Pin
10	GLV	Low-Side V-Phase Gate Pin
11	GLU	Low-Side U-Phase Gate Pin
12	SenLU	Low-Side U-Phase Sense Pin
13	SenHU	High-Side U-Phase Sense Pin
14	GHU	High-Side U-Phase Gate Pin
15	Vbat Sen	Vbat Sense Pin
16	Vbat Sen	Vbat Sense Pin (Shared: 15, 16)
17	VB	Battery Voltage Pin
18	GND	Ground Pin
19	U	U-Phase Output Pin
20	V	V-Phase Output Pin
21	W	W-Phase Output Pin

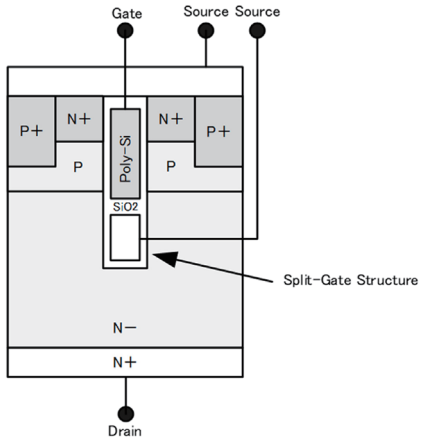

Figure 4. Cell Structure Diagram of ZeroMos

In addition to the VFP structure, optimization of cell pitch and implementation of wafer thinning technology further reduce on-resistance compared to conventional MOSFET structures. These improvements contribute to the miniaturization of the MOSFET chip and, consequently, the module package.

4.2 Built-in RC Filter Circuit

The product incorporates an RC filter circuit between VB and GND, composed of resistors and capacitors (see Figure 3). This filter effectively suppresses surge voltage, switching noise, and ringing. By integrating the filter circuit within the package, the need for external filtering on the customer side is reduced, contributing to cost savings.

4.3 Built-in Thermistor Function

The product includes a thermistor function between terminals 1 and 2. Customers require temperature monitoring close to the chip, and by integrating the thermistor within the package, early detection of abnormal heating and prevention of thermal damage to the system are made possible.

4.4 Adoption of High Heat Dissipation DBC Structure

The package employs a Direct Bonding Copper (DBC) structure with excellent heat dissipation properties, achieving low thermal resistance (see Table 2).

4.5 Package Design Changes from Previous Products

This product is based on the package design of the Company's previous automotive high-voltage three-phase brushless motor driver series, SAM470×× (DIP27). However, the DIP27 package could not accommodate the larger ZeroMos chip size.

To address this, the new package design retains the compact form factor of DIP27 while implementing the following changes:

- First, the staggered layout used to secure creepage distance for high-voltage applications was eliminated, as it is unnecessary for this low-voltage product (see Figure 5).
- Second, the internal stage for mounting a control chip (MIC), which was present in previous products, was removed since this product does not include a control chip.

These changes allowed for an expanded DBC substrate area, enabling the integration of the ZeroMos chip.

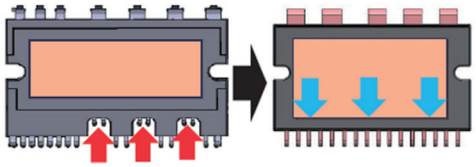

(a) Conventional Product Package (b) Newly Developed Product Package

Figure 5. Diagram of Changes from SAM470×× Package

5. Evaluation Results

This section presents selected evaluation results for the product currently under development.

5.1 Temperature Characteristics of $R_{DS(ON)}$

To verify the performance of the low on-resistance ZeroMos described in Section 4.1, temperature characteristics of $R_{DS(ON)}$ were measured and plotted (see Figure 6). The results confirmed that the $R_{DS(ON)}$ value at 25°C meets the specified requirements (see Table 2).

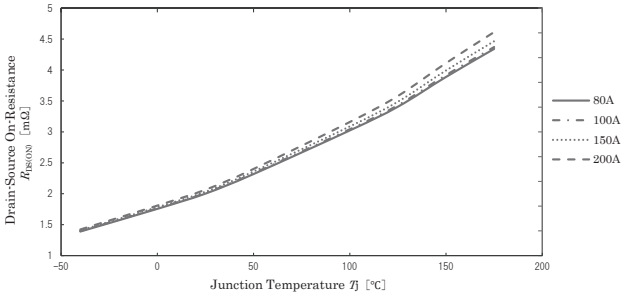

Conditions : Measurement Phase = Hi-Side V Phase, V_{GS} = 10V, I_D = 80A to 200A, T_j = −40°C to 175°C

Figure 6 Temperature Characteristics of $R_{DS(ON)}$

5.2 Effectiveness of RC Filter

To evaluate the effectiveness of the built-in RC filter described in Section 4.2, switching characteristics were compared with and without the filter. The results are shown in Figures 7 and 8.

The results showed improved ringing during both turn-off and turn-on operations, confirming the effectiveness of the RC filter.

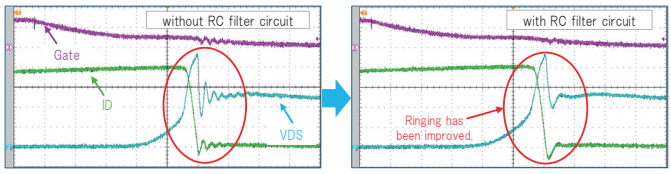

Conditions : Verification Phase = Low-Side V Phase, V_B = 48V, V_{GS} = 15V, Lp = 14μF, Ta = 25°C, Filter Constants = 2.2Ω + 0.047μF + 0.047μF (with and without)

Figure 7. Switching Waveform at Turn-Off

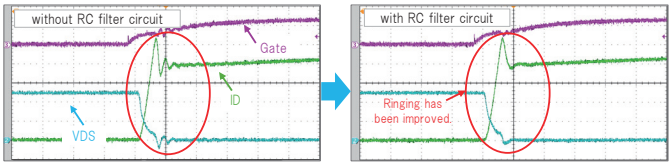

Conditions : Verification Phase = Low-Side V Phase, V_B = 48V, V_{GS} = 15V, Lp = 14μF, Ta = 25°C, Filter Constants = 2.2Ω + 0.047μF + 0.047μF (with and without)

Figure 8. Switching Waveform at Turn-On

5.3 Thermal Resistance Evaluation

To verify the performance of the high heat dissipation DBC substrate described in Sections 4.4 and 4.5, thermal resistance evaluation was conducted. The results are shown in Figure 9. Post-evaluation structural function analysis confirmed that the boundaries of grease and insulation sheet were clearly identified within the graph, indicating compliance with the specifications (see Table 2).

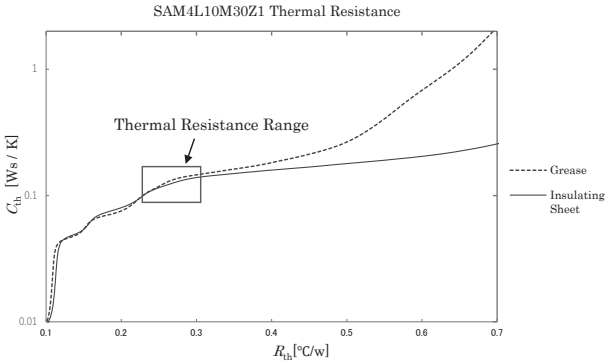

Conditions : Measurement Phase = Hi-Side W Phase,
Sample Mounting = Two Conditions : with Grease and with Insulating Sheet

Figure 9. Structure Function Graph

6. Conclusion

This paper introduced the product SAM4L10M30Z1, currently under development, and presented its evaluation results. The evaluation confirmed that the product meets its specifications. Reliability tests such as AQG324 and AEC101 are planned for future development.

The results of the current and upcoming evaluations will be reflected in product development to deliver higher-quality products to customers.

References

(1) MarkLines, “Forecast of Powertrain Composition Ratios in Global Light Vehicle Sales,” MarkLines Official Website, https://www.marklines.com/portal_top_ja.html

(2) Kondo, Tanaka: Sanken Technical Report, vol. 53, p.47, (November 2021)